The Journal of Immunology

The Cooperative Induction of Hypoxia-Inducible Factor-1 α and STAT3 during Hypoxia Induced an Impairment of Tumor Susceptibility to CTL-Mediated Cell Lysis

Muhammad Zaeem Noman, Stéphanie Buart, Jos Van Pelt, Catherine Richon, Meriem Hasmim, Nathalie Leleu, Wictoria Maria Suchorska, Abdelali Jalil, Yann Lecluse, Faten El Hage, Massimo Giuliani, Christophe Pichon, Bruno Azzarone, Nathalie Mazure, Pedro Romero, Fathia Mami-Chouaib and Salem Chouaib

J Immunol 2009; 182:3510-3521; ;
doi: 10.4049/jimmunol.0800854
http://www.jimmunol.org/content/182/6/3510

The Journal of Immunology is published twice each month by
The American Association of Immunologists, Inc.,
1451 Rockville Pike, Suite 650, Rockville, MD 20852

Print ISSN: 0022-1767 Online ISSN: 1550-6606.

The Cooperative Induction of Hypoxia-Inducible Factor-1α and STAT3 during Hypoxia Induced an Impairment of Tumor Susceptibility to CTL-Mediated Cell Lysis[1,2]

Muhammad Zaeem Noman,* Stéphanie Buart,* Jos Van Pelt,† Catherine Richon,* Meriem Hasmim,* Nathalie Leleu,* Wictoria Maria Suchorska,* Abdelali Jalil,* Yann Lecluse,‡ Faten El Hage,* Massimo Giuliani,§ Christophe Pichon,* Bruno Azzarone,§ Nathalie Mazure,¶ Pedro Romero,‖ Fathia Mami-Chouaib,* and Salem Chouaib[3]*

Hypoxia is an essential component of tumor microenvironment. In this study, we investigated the influence of hypoxia (1% PO_2) on CTL-mediated tumor cell lysis. We demonstrate that exposure of target tumor cells to hypoxia has an inhibitory effect on the CTL clone (Heu171)-induced autologous target cell lysis. Such inhibition correlates with hypoxia-inducible factor-1α (HIF-1α) induction but is not associated with an alteration of CTL reactivity as revealed by granzyme B polarization or morphological change. Western blot analysis indicates that although hypoxia had no effect on p53 accumulation, it induced the phosphorylation of STAT3 in tumor cells by a mechanism at least in part involving vascular endothelial growth factor secretion. We additionally show that a simultaneous nuclear translocation of HIF-1α and phospho-STAT3 was observed. Interestingly, gene silencing of STAT3 by small interfering RNA resulted in HIF-1α inhibition and a significant restoration of target cell susceptibility to CTL-induced killing under hypoxic conditions by a mechanism involving at least in part down-regulation of AKT phosphorylation. Moreover, knockdown of HIF-1α resulted in the restoration of target cell lysis under hypoxic conditions. This was further supported by DNA microarray analysis where STAT3 inhibition resulted in a partly reversal of the hypoxia-induced gene expression profile. The present study demonstrates that the concomitant hypoxic induction of phopho-STAT3 and HIF-1α are functionally linked to the alteration of non-small cell lung carcinoma target susceptibility to CTL-mediated killing. Considering the eminent functions of STAT3 and HIF-1α in the tumor microenvironment, their targeting may represent novel strategies for immunotherapeutic intervention. *The Journal of Immunology,* **2009, 182: 3510–3521.**

Cytotoxic T lymphocytes are important effector cells in tumor rejection and have been described to play a crucial role in host defense against malignancies in both mouse and human (1). The major effector function of CTL is mediated through directional exocytosis of cytotoxic granules, primarily containing perforin and granzymes, into the target leading to cell death (2, 3). It is established that their antitumor response is regulated at several effector-target interaction levels involving both intracellular and extracellular stimuli (3). Accumulating evidence indicated that tumor cells play a crucial role in the control of immune protection (4) and contain many overlapping mechanisms to maintain their functional disorder and evasion. In this regard, it has been suggested that tumor cell growth in vivo is not only influenced by CTL-tumor cell interaction but also by tumor susceptibility to cell-mediated death (5). Even though the resistance of tumor cells to cell-mediated cytotoxicity remains a drawback in the immunotherapy of cancer, its molecular basis is poorly understood. A great deal of effort has been focused on trying to understand the tumor escape to immune surveillance and to understand the molecular basis of tumor tolerance.

Several reports indicated that tumor cells evade adaptive immunity by a variety of mechanisms, including development of hypoxia (low oxygen tension) (6), and that the adaptation of these cells to an hypoxic environment results in an aggressive and metastatic cancer phenotype associated with a poor treatment outcome (7). Hypoxic microenvironments are frequent characteristics of solid tumors and are the consequences of morphologically and functionally inappropriate neovascularization, irregular blood flow, anemia, and high oxygen consumption of rapidly proliferating malignant cells. Solid tumors characteristically contain areas of hypoxia, which is a powerful stimulus for the expression of genes involved in proliferation, glycolysis, and angiogenesis (8). The molecular signaling pathways mediating gene induction by hypoxia have been elucidated and extensively reviewed (9). Hypoxia-inducible

*Institut National de la Santé et de la Recherche Médicale (INSERM) Unité 753, Villejuif, France; †Department of Hepatology, University Hospital Gasthuisberg, Leuven, Belgium; ‡Institut Gustave Roussy PR2, Villejuif, France; §INSERM, Unité Mixte de Recherche (UMR) 542, Université de Paris XI, Hôpital Paul Brousse, Villejuif, France; ¶Institute of Signalling, Developmental Biology and Cancer Research, Centre National de la Recherche Scientifique UMR 6543, Nice, France; and ‖Division of Clinical Onco-Immunology, Ludwig Institute for Cancer Research, Lausanne, Switzerland

Received for publication March 14, 2008. Accepted for publication January 8, 2009.

The costs of publication of this article were defrayed in part by the payment of page charges. This article must therefore be hereby marked *advertisement* in accordance with 18 U.S.C. Section 1734 solely to indicate this fact.

[1] This work was supported in part by grants from Institut National de la Santé et de la Recherche Médicale, Association pour la Recherche sur le Cancer (ARC) (no. 3272), and Ligue contre le Cancer (comité de Seine Saint-Denis), as well as Institut National du Cancer (INCA), ARC/INCA, and Agence Nationale de la Recherche.

[2] Microarray Data deposition: The detailed microarray data related to this paper have been submitted to the Array Express data repository at the European Bioinformatics Institute (www.ebi.ac.uk/arrayexpress; accession no. E-TABM-611).

[3] Address correspondance and reprint request to Dr. Salem Chouaib, Institut National de la Santé et de la Recherche Médicale Unité 753, Institut Gustave Roussy, 39 rue Camille Desmoulins, F-94805 Villejuif, France. E-mail address: chouaib@igr.fr

www.jimmunol.org/cgi/doi/10.4049/jimmunol.0800854

factor-1 (HIF-1)[4] is an $\alpha_1\beta_1$ heterodimer specifically recognizing hypoxia-response elements of oxygen-regulated genes. Several studies have shown that under hypoxic conditions, HIF-1α becomes constitutively up-regulated in many cancer types and plays a major role in tumor progression, mostly as a result of inhibition of protein degradation. In response to physiological hypoxia, HIF-1α becomes rapidly stabilized and is localized to the nucleus, where it specifically binds to a short DNA sequence (HREs, hypoxia response elements), thereby controlling the transcription of many genes that are critical for continued cellular function under hypoxic conditions (10, 11). Whereas the potential involvement of this factor in mediating resistance to radiation and drug therapy (12, 13) has been reported, the mechanisms underlying this resistance still need deeper understanding. Although the resistance of hypoxic cells to killing and the aggressiveness of highly hypoxic tumors are, in part, due to the overexpression of HIF-1α (14, 15), the consequences of HIF-1α induction on specific lysis of human tumor cells by CTL remain unknown. Therefore, since hypoxia is a common feature of solid tumors and one of the hallmarks of tumor microenvironment, we asked whether hypoxia confers tumor resistance to CTL-mediated killing.

While numerous findings provided compelling evidence that a causal relationship exists between STAT3 activation and HIF-1α-dependent angiogenesis (16), their relationship in regulating tumor cell susceptibility to CTL-mediated specific lysis under hypoxic conditions is not yet known. There is strong evidence that STAT3 contributes to malignant transformation and progression by transactivation of host target genes involved in fundamental events of tumor development, including proliferation, survival, self-renewal, invasion, and angiogenesis (17–19). STAT3 is critical for these processes, because its inhibition by a variety of means can exert an anticancer progression (20). In this context, STAT3 signaling has been shown to inhibit apoptosis and to induce a more aggressive phenotype through the activation of specific signaling pathways (21).

The primary focus of the current study was to examine the impact of hypoxia on specific lysis of tumor cells by CTL. Our results show that the cooperative induction of STAT3 and HIF-1α is functionally linked to the acquisition of tumor cell resistance to CTL-mediated killing under hypoxic conditions by autologous CTL. Targeting STAT3 resulted in a significant attenuation of this resistance, thus providing a lead for therapeutic modulation of hypoxia-mediated immunoresistance.

Materials and Methods

Reagents and Abs

Protease inhibitors were purchased from Roche Applied Science. Bicinchoninic acid protein assay reagent was obtained from Pierce. CHAPS was obtained from Sigma-Aldrich. For the detection of HIF-1α protein, two different Abs were used. For confocal microscopy, anti-HIF-1α (antiserum 2087) as previously described (22) was used. For Western blots, HIF-1α Ab (BD Transduction Laboratories) was purchased. Abs against STAT3 and phospho-STAT3 (p-STAT3) were purchased from Cell Signaling Technology. Actin (clone c-11) and Abs against p53, AKT and p-AKT were purchased from Santa Cruz Biotechnology. Cucurbitacin I (CCB-I) (JSI-124; National Cancer Institute NCI identifier: NSC 521777) was purchased from Indofine Chemical and kept as a stock solution of 50 mM in DMSO. Avastin (Bevacizumab) was purchased from Genentech.

[4] Abbreviations used in this paper: HIF-1, hypoxia-inducible factor-1; CCB-I, cucurbitacin-I; MHC-I, MHC class I; NSCLC, non-small cell lung cancer; p-STAT3, phospho-STAT3; PKB (also called AKT), protein kinase B; RNAi, RNA interference; siRNA, small interfering RNA; VEGF, vascular endothelial growth factor.

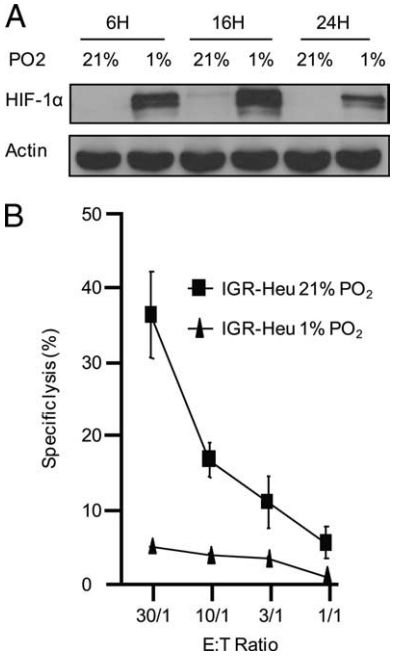

FIGURE 1. Hypoxic stress on IGR-Heu tumor cells induces HIF-1α and decreases susceptibility to CTL (Heu171)-mediated lysis. *A*, IGR-Heu tumor cells were incubated in normoxia (21% PO_2) and hypoxia (1% PO_2) for different time intervals. After hypoxic exposure, whole-cell lysates (30 μg) were subjected to SDS-PAGE, blotted, and probed with Abs, as indicated. Actin was used as the loading control. *B*, The consequence of hypoxic stress on IGR-Heu tumor cells to CTL-mediated lysis was studied. IGR-Heu tumor cells were incubated in normoxia (21% PO_2) and hypoxia (1% PO_2) for 16 h. Cytotoxicity was determined by a conventional 4-h ^{51}Cr release assay at different ratios. Heu171 (TIL-derived T cell clone) was used as effectors. Bars, SD.

Culture of tumor cells and CTL

The IGR-Heu lung carcinoma cell line was derived and maintained in culture as described previously (23). Heu171 cell clone was derived from autologous TIL (24, 25). IGR-Heu lung carcinoma cell line was grown in DMEM/F12 medium supplemented with 10% FCS (Seromed), 1% Ultroser G (Life Technologies), 1% penicillin-streptomycin, and 1 mM sodium pyruvate.

Hypoxia treatment and HIF-1α induction

For the induction of HIF-1α, cell cultures were incubated in a hypoxia chamber ($InVivo_2$ 400 Hypoxia Workstation; Ruskinn) in a humidified atmosphere containing 5% CO_2 and 1% O_2 at 37°C (26). Once hypoxic conditions were optimized, cells were always exposed to the same optimized hypoxic conditions (1% O_2, 5% CO_2, and 94% N_2) at 37°C (16 h) for the optimal induction of HIF-1α. Cell culture medium and cells for protein analysis were harvested while in the hypoxia workstation and were not reoxygenated before harvesting.

Cytotoxicity assay

The cytotoxic activity of the CTL clone (Heu171) was measured by a conventional 4-h ^{51}Cr release assay by using triplicate cultures in round-bottom 96-well plates. Different E:T ratios were used. Briefly, E:T ratios 30:1, 10:1, 3:1, and 1:1 were used on 1000 target cells per well, and after 4 h of coculture at 37°C, the supernatants were transferred to LumaPlate 96 wells (PerkinElmer), dried down, and counted on a Packard's TopCount NXT. Percent-specific cytotoxicity was calculated conventionally as described earlier (27). All cytotoxicity experiments with ^{51}Cr were performed under normoxic conditions.

TNF production assay

TNF-β release was measured as described previously (28); briefly, TNF-β was detected by measuring the cytotoxicity of the culture medium on the TNF-sensitive WEHI-164c13 cells, with an MTT colorimetric assay.

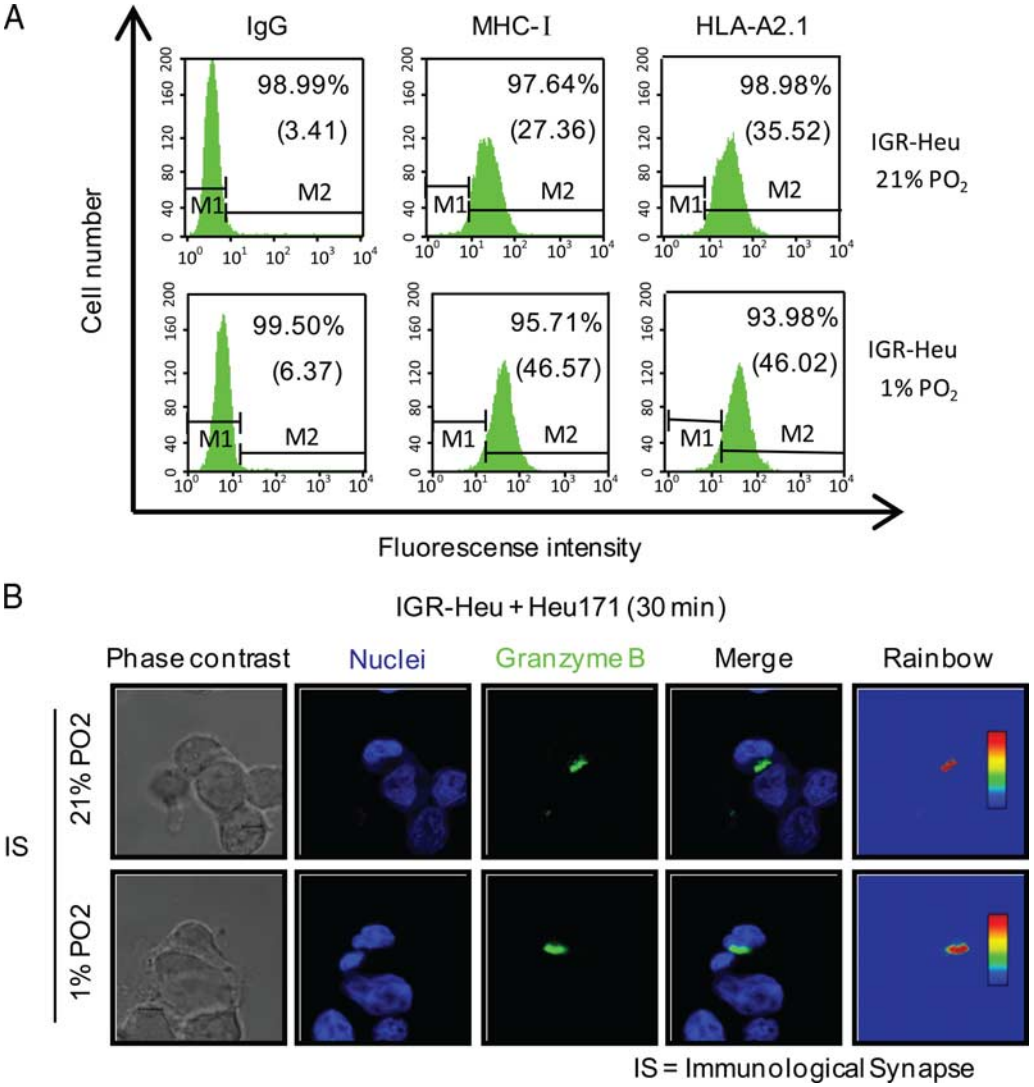

FIGURE 2. Hypoxic stress on IGR-Heu tumor cells does not affect CTL priming and cell morphology. *A*, Analysis of surface expression of HLA class I (MHC-I) and HLA-A2.1 was conducted on IGR-Heu tumor cells kept in normoxia (21% PO_2) and hypoxia (1% PO_2) for 16 h. Isotypic control mAb was included (IgG). *B*, Confocal microscopy analysis of granzyme B polarization in the contact area between tumor cells and CTL clone. IGR-Heu tumor cells were placed in normoxia (21% PO_2) and hypoxia (1% PO_2), followed by immunofluorescence staining with Abs recognizing granzyme B. Nuclei were counterstained with To-Pro-3 iodide. The confocal scanning fluorescence micrographs shown are representative of most of the cells analyzed (blue, nucleus; green, granzyme B). *C*, Hypoxic stress had no effect on tumor cell morphology. IGR-Heu tumor cells were placed in normoxia (21% PO_2) and hypoxia (1% PO_2) for 16 h. Immunofluorescence staining for phalloidin was done with appropriate Ab. Nuclei were counterstained with To-Pro-3 iodide. The confocal scanning fluorescence micrographs shown are representative of most of the cells analyzed (green, phalloidin). *D*, TNF-β production by the autologous T cell clone in response to IGR-Heu stimulation. CTL clone Heu171 was cocultured in the presence of IGR-Heu cells placed in normoxia (21% PO_2) and hypoxia (1% PO_2) for 24 h. The amount of TNF-β produced by the CTL clone was measured using the TNF-sensitive WEHI-164c13 cells. Bars, SD. *E*, Viability of IGR-Heu tumor cells under hypoxic and normoxic conditions. IGR-Heu tumor cells were placed in normoxia (21% PO_2) and hypoxia (1% PO_2) for 16 h. Apoptosis was assessed by Annexin V^{FITC}/propidium iodide staining.

RNA interference (RNAi)

Gene silencing of STAT3 and HIF-1α expression by the IGR-Heu cell line was performed by using chemically synthesized, double-stranded small interfering RNA (siRNA). STAT3 siRNA was obtained from Santa Cruz Biotechnology (sc-29493), which is a pool of three target-specific 20–25 nt siRNA designed to knock down gene expression (29). HIF-1α siRNA was purchased from Invitrogen Life Technologies (Validated stealth RNAi DuoPak ref 1299003). Luciferase siRNA (siRNA duplex, C G U A C G C G G A A U A C UU C G A dTdT, and U C G A A G U A U U C C G C G U A C G dTdT), included as a negative control, was purchased from Sigma-Proligo. Briefly, cells were transfected by electroporation with 50 nM siRNA in a gene Pulser Xcell electroporation system (Bio-Rad) at 300 V and 500 μF, using electroporation cuvettes (Eurogentec) and then allowed to grow for 72 h (30).

Confocal microscopy

For confocal microscopy analysis of localization of HIF-1α and p-STAT3, IGR-Heu tumor cells were plated on poly-L-lysine-coated coverslips (Sigma-Aldrich) in 6-well plates at a density of 5×10^4 cells/well and incubated for 16 h at 37°C in two different conditions: normoxia (21% PO_2) and hypoxia (1% PO_2). Afterward, cells were washed once with PBS, fixed with 4% paraformaldehyde for 1 h, and permeabilized with ice-cold 100% methanol at −20°C for 10 min. Cells were then blocked with 10% FBS for 20 min. Immediately after blocking, fixed cells were stained first with either anti-p-STAT3 or anti-HIF-1α primary Ab and afterward with a secondary Ab coupled to biotin (GAR IgG H+L biotin-xx; Molecular Probes) for 1 h. At last, cells were incubated with streptavidin Alexa Flour 488 (Molecular Probes) for 1 h. All Abs were diluted in PBS containing 1 mg/ml BSA. Nuclei were stained with TO-PRO-3 iodide (Invitrogen).

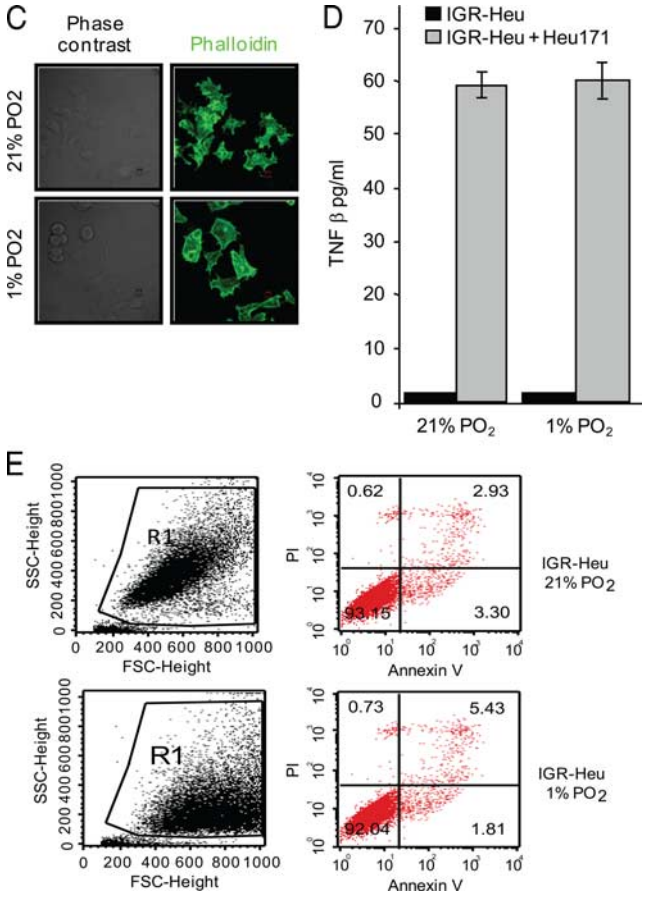

FIGURE 2. (*continued*)

Coverslips were mounted with Vectashield (Vector Laboratories) and analyzed using a fluorescence microscope (LSM-510; Carl Zeiss Micro Imaging) as described previously (31, 32).

IL-6, IL-10, and vascular endothelial growth factor (VEGF) ELISA

IL-6, IL-10, and VEGF protein levels were assessed using ELISA. IGR-Heu tumor cells were grown in 6-well plates (DMEM supplemented with 10% FBS) until they had reached 50–60% confluency. The media were then replaced with DMEM supplemented with 0.5% FBS. These cells were then kept under normoxia (21% PO_2) and hypoxia (1% PO_2) for an additional 24 h, whereupon their media were collected, filter sterilized, aliquoted, and stored at −80°C. Secretion of IL-6, IL-10, and VEGF was quantified using ELISA kits obtained from R&D Systems (catalog nos. D6050, D1000B, and DVE00, respectively). Each assay was performed per the manufacturer's instructions. Samples were assayed in triplicates. Error bars represent ± SD.

Flow cytometry analysis

Flow cytometry analysis was performed by using a FACSCalibur flow cytometer. Data were processed using CellQuest software (BD Biosciences). Anti-HLA-A2.1 (MA2.1), anti-HLA class I, or MHC class I (MHC-I) (W6/32) were used as reported previously (28). For apoptosis evaluation, the Annexin V^{FITC}/propidium iodide assay kit (BD Biosciences) was used according to the standard protocol.

Western blotting

Western blotting was performed as reported previously (32, 33). Briefly cells were grown in two different conditions normoxia (21% PO_2) and hypoxia (1% PO_2) for 16 h at 37°C. Cells were scrapped off, lysed in an appropriate buffer containing 20 mM Tris-HCl (pH 7.5), 1% CHAPS, 150 mM NaCl, 10% glycerol, 1 mM Na_3VO_4, and a commercial protease inhibitor mixture (Complete Protease Inhibitor Mixture; Roche Molecular Biochemicals). Cells were then placed on ice for 30 min, centrifuged at 10,000 × *g* for 30 min at 4°C, and their supernatants were collected. Thirty micrograms of total protein extracts were resolved on 8 or 12% SDS-polyacrylamide gels. Proteins were transferred onto nitrocellulose membrane by wet method, and unspecific binding sites were blocked with 3% milk/Tween 20 Tris-buffered saline (TTBS; 50 mM Tris HCl, 140 mM NaCl, and 0.05% Tween 20 (pH 7.2)) for 1 h. The primary Abs were added at a dilution of 1/1000 and incubated overnight at 4°C. Afterward, nitrocellulose membranes were washed three times for 5 min each with TTBS. For protein detection, blots were incubated with a HRP-labeled anti-mouse or anti-rabbit secondary Abs for 1 h at a dilution of 1/2000 and washed three times for 5 min each with TTBS, followed by ECL detection analysis. Correction for background was performed with NIH Image software.

Microarray analysis

DNA Microarray was performed using (Agilent Human Whole Genome Microarray: 44,000 spots) as previously reported (30) under two different conditions, hypoxia vs normoxia (Hypo Normo) and siRNA STAT3 vs siRNA-Luc (STAT3 CT) by using (Agilent Human Whole Genome Microarray: 44,000 spots). In both conditions, total RNA was extracted and compared by using Agilent oligonucleotide dual-color technology, running dye swap and duplicate experiments. Probe synthesis and labeling were performed by Agilent's Low Fluorescent Low Input Linear Amplification Kit. Hybridization was performed on human whole-genome 44,000 oligonucleotide microarrays (Agilent) by using reagents and protocols provided by the manufacturer. Feature extraction software provided by Agilent (version 7.5) was used to quantify the intensity of fluorescent images and to normalize results using the linear and lowess subtraction method. Primary analysis was performed by using Resolver software (Rosetta Laboratories) to identify genes differentially expressed between resistant and sensitive cell lines (IGR-Heu/IGR HeuR8) with a fold change > 2 and a value of $p < 10^{-5}$. For additional analysis, we used the GenMapp/Mapfinder software package (www.genmapp.org; Gladstone Institute, University of California San Francisco).

Results

Hypoxic stress-induced HIF1α is associated with a decrease in CTL-mediated tumor cell lysis

Hypoxia is a specific property of solid tumors and has been widely documented to contribute to low apoptotic potential. To investigate the influence of hypoxic stress on human tumor cell susceptibility to CTL-mediated killing, we used the human non-small cell lung carcinoma (NSCLC) cell line IGR-Heu and the autologous CTL clone (Heu171), recognizing a mutated α-actinin-4 peptide in an HLA-A2.1 context. As previously described, IGR-Heu cells were lysed by the CTL clone through the perforin/granzymes pathway (23, 34, 35). Because cancer cells can adapt to hypoxia primarily through a transcriptional response pathway mediated by the HIF-1-α, its induction in IGR-Heu cells under hypoxic conditions (1% PO_2) was first determined. As depicted in Fig. 1*A*, Western blot analysis shows a HIF-1α induction upon culture of IGR-Heu under hypoxic conditions. Kinetic analysis indicated that optimal induction was obtained after 16 h of cell culture under hypoxic conditions. Such an induction was associated with a dramatic decrease (80% inhibition at E:T ratio of 30:1) in CTL-mediated IGR-Heu killing (Fig. 1*B*). These results indicate that hypoxic tumor cells are less susceptible to lysis induced by the autologous CTL clone.

Hypoxic stress does not affect CTL reactivity and tumor cell morphology

To determine whether hypoxic stress-induced alteration of target susceptibility to CTL-mediated lysis involves an alteration in CTL reactivity or a change in tumor cell morphology, we have examined the influence of hypoxia on MHC-I molecule expression using cytometry analysis and specific Abs. As shown in Fig. 2*A*, no difference in staining with W6/32 (HLA class I specific) and MA2.1 (specific for HLA-A2) Abs was observed on hypoxic cells (1% PO_2) as compared with cells

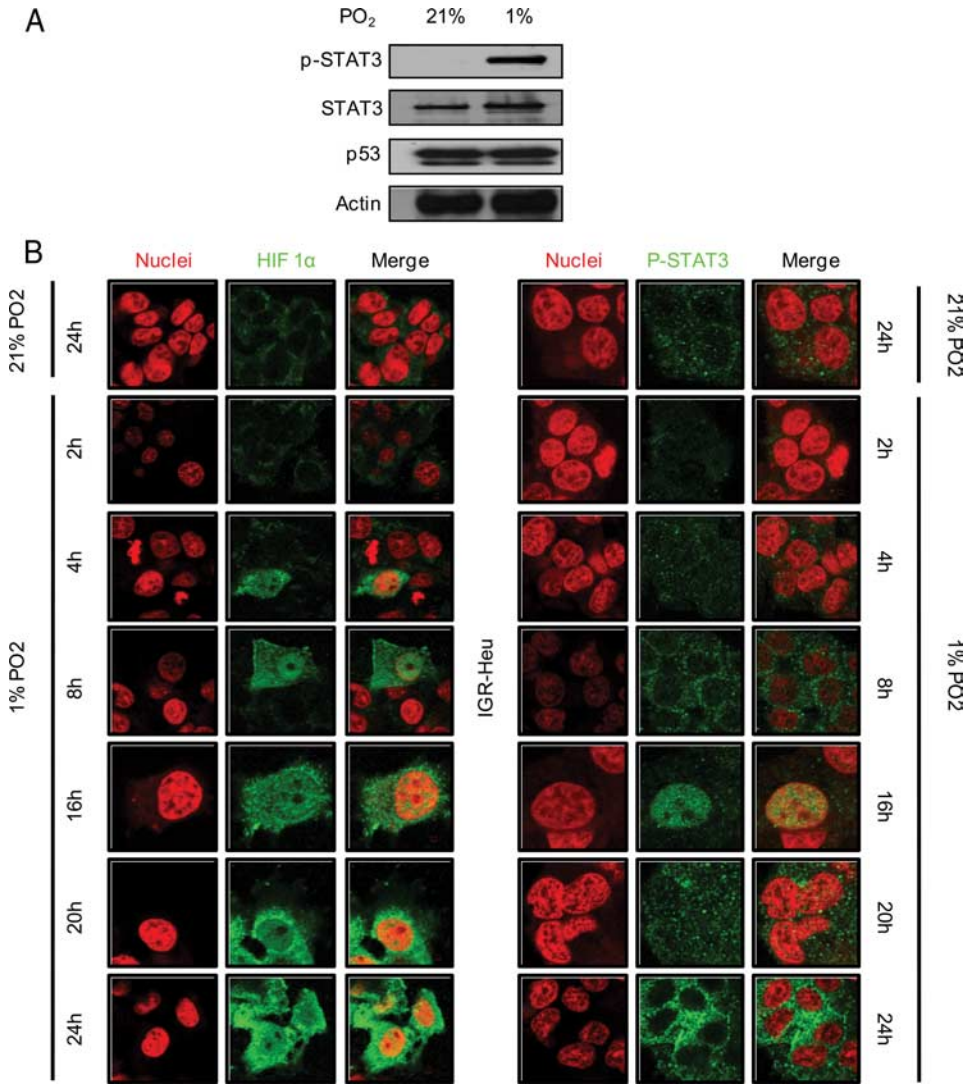

FIGURE 3. Hypoxic stress on IGR-Heu tumor cells induced phosphorylation of STAT3 and simultaneous nuclear translocation of HIF-1α and p-STAT3. *A*, IGR-Heu tumor cells were kept in normoxia (21% PO_2) and hypoxia (1% PO_2). After 16 h of incubation, whole-cell lysates (30 μg) were subjected to SDS-PAGE, blotted, and probed with Abs, as indicated. Actin was used as the loading control. *B*, Confocal microscopy analysis for nuclear translocation of HIF-1α and p-STAT3. IGR-Heu tumor cells were placed in normoxia (21% PO_2) and hypoxia (1% PO_2), followed by immunofluorescence staining with Abs recognizing HIF-1α and p-STAT3. A time course study was done to follow the cytoplasmic localization and, eventually, the hypoxia-mediated nuclear translocation of HIF-1α and p-STAT3. It was observed that both HIF-1α and p-STAT3 translocated in the nucleus after 16 h of hypoxia. Nuclei were counterstained with To-Pro-3 iodide. The confocal scanning fluorescence micrographs shown are representative of most of the cells analyzed (blue, nucleus; green, HIF-1α and p-STAT3).

cultured under normoxic conditions (21% PO_2). To examine the recognition of hypoxic cells by the CTL clone, we examined the reactivity of the CTL clone to hypoxic autologous target. Confocal microscopy analysis shown in Fig. 2*B* indicates the polarization of cytotoxic granules as defined by granzyme B accumulation in the contact area between the CTL clone and hypoxic or normoxic IGR-Heu tumor cells. This indicates that hypoxic tumor cells are efficient in triggering the reactivity of the specific CTL clone that was further confirmed by TNF secretion assay (Fig. 2*D*).

Because we have recently provided evidence that a change in tumor cell morphology could lead to a decrease in their susceptibility to CTL-induced tumor cell death (30), we asked whether the inhibitory effect of hypoxia involves a tumor cell morphological change that would be associated with the observed alteration of their killing by Heu171 CTL clone. Results of confocal microscopy analysis shown in Fig. 2*C* indicate that the acquisition of resistance to CTL following treatment of target cells with hypoxic stress did not result in tumor cell morphological changes since F-actin content, as revealed by Alexa Fluor 568-phalloidin staining, was similar in hypoxic and normoxic cells. This rules out that the acquisition of hypoxic tumor resistance to CTL-mediated killing might result from a shift in the level of actin polymerization. Furthermore, as depicted in Fig. 2*E*, the hypoxic stress had no effect on IGR-Heu viability as revealed by annexin V/propidium iodide staining.

STAT3 phosphorylation in tumor cells under hypoxic conditions correlates with the acquisition of resistance to CTL-induced lysis

The interaction of STAT3 with HIF-1α was identified in hypoxic tumor cells (16). Therefore, we wished to delineate the respective involvement of these factors in the regulation of target cell susceptibility to specific lysis. For this purpose, total extracts of IGR-Heu cultured under hypoxic or normoxic conditions were subjected to Western blot analysis. While under hypoxic conditions, a dramatic increase in STAT3 phosphorylation was observed; there was no effect on the tumor suppressor protein p53 (Fig. 3*A*) and survivin (data not shown). Next, we examined the temporal kinetics of HIF-1α and STAT3 nuclear translocation in IGR-Heu cultured under hypoxic conditions from 2 to 20 h using confocal microscopy. Data shown in Fig. 3*B* indicate that at least 16 h of hypoxic treatment are required for nuclear translocation of both HIF-1α and STAT3. In fact, before 16 h both HIF-1α and STAT3 are predominantly present in the cytosol. At 16 h, the hypoxic cells exhibited an optimal HIF-1α and STAT3 accumulation in the nucleus.

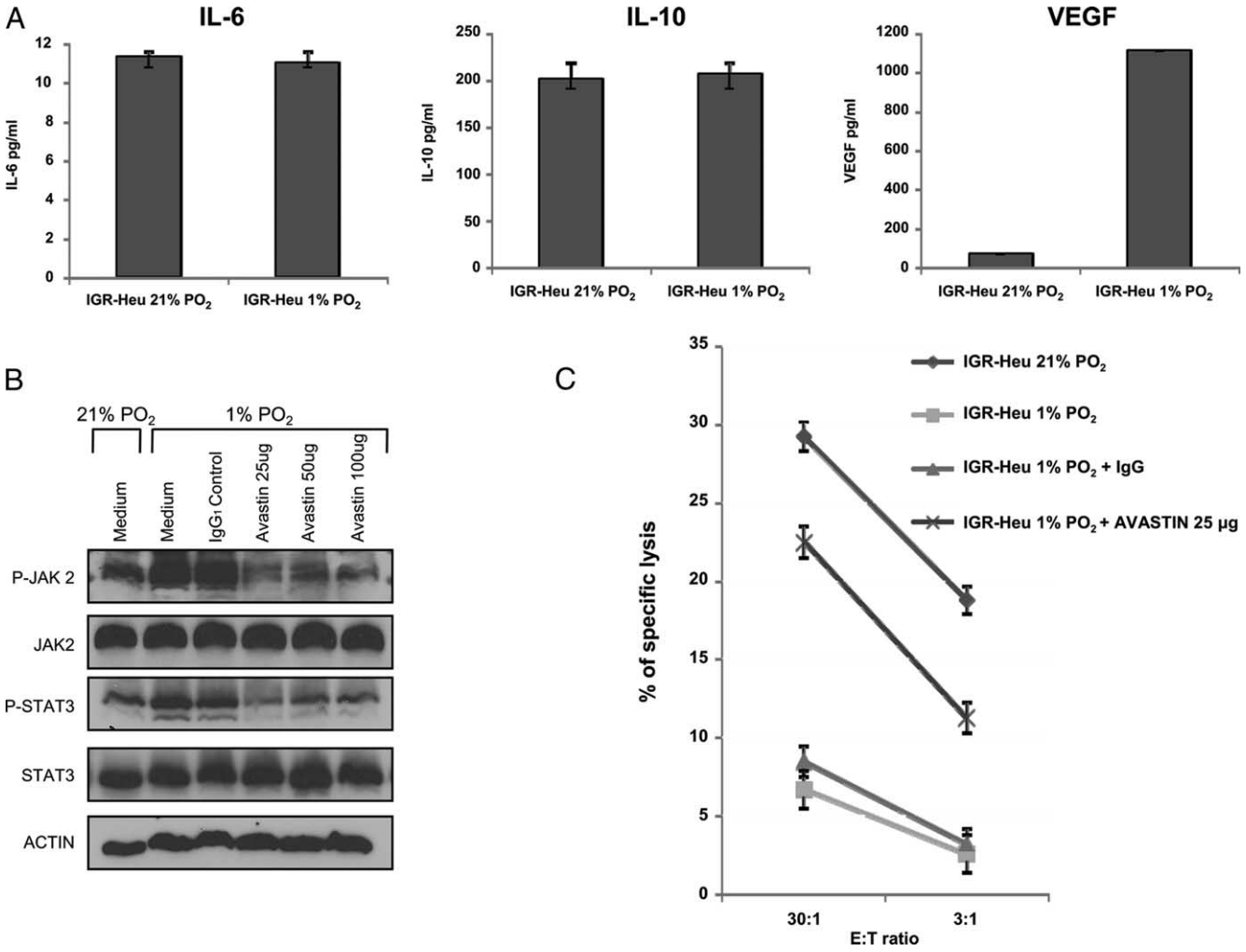

FIGURE 4. Involvement of VEGF in STAT3 activation under hypoxia and relationship with JAK/STAT3 pathway. *A*, IGR-Heu tumor cells were kept under normoxia (21% PO_2) and hypoxia (1% PO_2) for 24 h. ELISA was performed for quantification of IL-6, IL-10, and VEGF by Quantikine Human immunoassay R&D Systems. Bars, SD. The results shown are representative of two independent experiments. *B*, IGR-Heu tumor cells were incubated for 24 h with 25, 50, and 100 μg/ml Avastin (Genentech) or an isotype control Ab (human IgG1; Sigma-Aldrich) in reduced serum conditions (0.5% FBS) under (21% PO_2) and hypoxia (1% PO_2). Whole-cell lysates (30 μg) were subjected to SDS-PAGE, blotted, and probed with Abs, as indicated. Actin was used as the loading control. *C*, Attenuation of IGR-Heu tumor cells resistance to CTL (Heu171)-mediated lysis under hypoxic conditions following treatment with anti-VEGF (Avastin). IGR-Heu tumor cells were incubated for 24 h with 25 μg/ml Avastin or an isotype control Ab (human IgG1; Sigma-Aldric h) under normoxia (21% PO_2) and hypoxia (1% PO_2). Cytotoxicity was determined by a conventional 4-h ^{51}Cr release assay. Heu171 (TIL-derived T cell clone) was used as effectors. Bars, SD.

Hypoxia-induced phosphorylation of STAT3 is associated with induction of VEGF

The role of hypoxia in controlling the activation of STAT3 in tumor cells is not fully understood. Soluble factors like IL-6, IL-10, and VEGF are known to induce activation of STAT3 through JAK/STAT3 pathway (36), and furthermore, autocrine and paracrine IL-6 has been shown to activate STAT3 via IL-6/JAK pathway (37). Therefore, we investigated the role of these mediators in activating JAK/STAT3 pathway under hypoxic conditions. As depicted in Fig. 4*A*, 24-h hypoxic conditioning (1% PO_2) of IGR-Heu tumor cells does not alter their production of IL-6 and IL-10. However, a 16-fold increase in the production of VEGF under hypoxia was observed.

To determine the role of VEGF in modulating the hypoxic activation of STAT3, we incubated IGR-Heu tumor cells with different concentrations of anti-VEGF (Avastin) under normoxia (21% PO_2) and hypoxia (1% PO_2) for 24 h. Using Western blot analysis, we found that the neutralization of VEGF by Avastin under hypoxic stress resulted in a dramatic inhibition of p-STAT3. This VEGF-mediated p-STAT3 inhibition was also associated with an inhibition of p-JAK2 (Fig. 4*B*). These observations indicate that VEGF is involved in the control of hypoxic induction of p-STAT3 through an autocrine mechanism involving JAK/STAT3 pathway.

To find out the potential involvement of hypoxia-induced VEGF in modulating the tumor cell susceptibility to CTL-mediated lysis via p-STAT3, we incubated IGR-Heu tumor cells for 24 h with 25 μg/ml Avastin or an isotype control Ab human IgG1 under normoxia (21% PO_2) and hypoxia (1% PO_2). Data depicted in Fig. 4*C* indicate a remarkable increase in CTL-mediated killing of anti-VEGF (Avastin)-treated cells as compared with control cells. This finding further strengthens the notion that the activation of STAT3 via VEGF-JAK/STAT3 autocrine loop plays an essential part in the acquisition of tumor cell resistance to CTL-induced killing under hypoxic conditions.

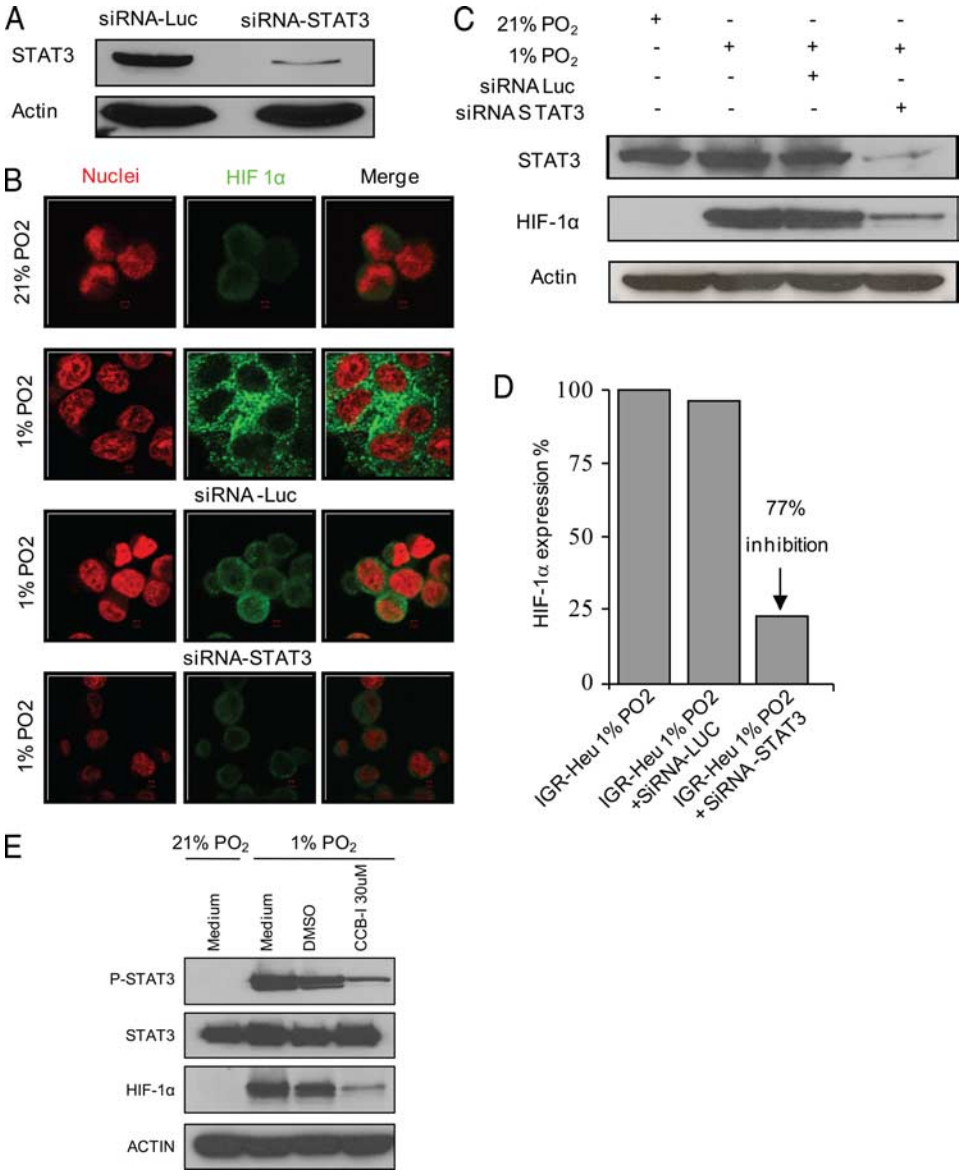

FIGURE 5. Gene silencing of STAT3 and pharmacological inhibition of p-STAT3 resulted in HIF-1α inhibition. *A*, Knockdown of STAT3 expression. IGR-Heu tumor cells were transfected with siRNA STAT3 or control siRNA-luciferase. Seventy-two hours after transfection, whole-cell lysates (30 μg) were subjected to SDS-PAGE, blotted, and probed with Abs, as indicated. Actin was used as the loading control. *B*, Confocal microscopy analysis of localization of HIF-1α. IGR-Heu tumor cells were placed in normoxia (21% PO_2) and hypoxia (1% PO_2), followed by immunofluorescence staining with Abs recognizing HIF-1α. Nuclei were counterstained with To-Pro-3 iodide. The confocal scanning fluorescence micrographs shown are representative of most of the cells analyzed (blue, nucleus; green, HIF-1α). *C*, Western blots analysis of HIF-1α following the knockdown of STAT3 by siRNA. Actin was used as a loading control. *D*, Densitometry analysis of HIF-1α inhibition using Image J. *E*, CCB-I-mediated inhibition of p-STAT3 under hypoxic stress is associated with inhibition of HIF-1α. IGR-Heu tumor cells were incubated under normoxia (21% PO_2) and hypoxia (1% PO_2) (medium, a volume equivalent of DMSO and along with 30 μM CCB-I) for 6 h. Afterward, whole-cell lysates (30 μg) were subjected to SDS-PAGE, blotted, and probed with Abs, as indicated. Actin was used as a loading control.

Silencing of STAT3 in hypoxic tumor cells resulted in HIF-1α inhibition

To further assess the putative hypoxia-induced functional interaction between HIF-1α and STAT3 in the regulation of IGR-Heu susceptibility to CTL-mediated killing, transfection of hypoxic IGR-Heu with siRNA-targeting STAT3 was performed. The inhibition of STAT3 in hypoxic tumor cells was confirmed by Western blot analysis, showing that an efficient and specific knockdown of the levels of STAT3 protein was obtained. In contrast, luciferase siRNA (siRNA-Luc), used as a control, had no effect on STAT3 protein levels (Fig. 5*A*).

Because STAT3 has been reported to modulate the stability and the activity of HIF-1α in tumor cells (16), we assessed whether such an interplay exists in NSCLC. Results of confocal microscopy depicted in Fig. 5*B* indicate that the induction of HIF-1α in NSCLC hypoxic cells was dramatically inhibited in STAT3 siRNA-treated cells as compared with the control cells transfected with siRNA-Luc. These results were further confirmed by Western blot analysis (Fig. 5*C*), indicating a significant inhibition (77%) of HIF-1α after gene silencing of STAT3 as revealed by densitometry (Fig. 5*D*).

Pharmacological inhibition of STAT3 phosphorylation in hypoxic tumor cells resulted in the inhibition of HIF-1α induction under hypoxic stress

Although STAT3 has been reported to modulate the stability and activity of HIF-1α in tumor cells (16), the relationship between hypoxic induction of HIF-1α and STAT3 activation remains to be elucidated. For this purpose, we used CCB-I, known to specifically inhibit STAT3 activation in various human cancer cell lines and, more importantly, to inhibit the tumor growth in mice models (38).

Western blot analysis indicate that the CCB-I treatment of IGR-Heu tumor cells resulted in an inhibition of p-STAT3 in a dose-dependent manner under hypoxic conditions (Fig. 5*E*). As depicted in the figure, the inhibition of P-STAT3 was accompanied by an inhibition of HIF-1α induction by the hypoxic stress

RNAi-mediated knockdown of STAT3 increased hypoxic target susceptibility to CTL-induced killing

To gain insight into the potential role of STAT3 in the regulation of hypoxic target cell susceptibility to CTL-mediated lysis, the ability of CTL to kill STAT3-siRNA-transfected IGR-Heu cells treated with hypoxia was evaluated. Interestingly, as shown in

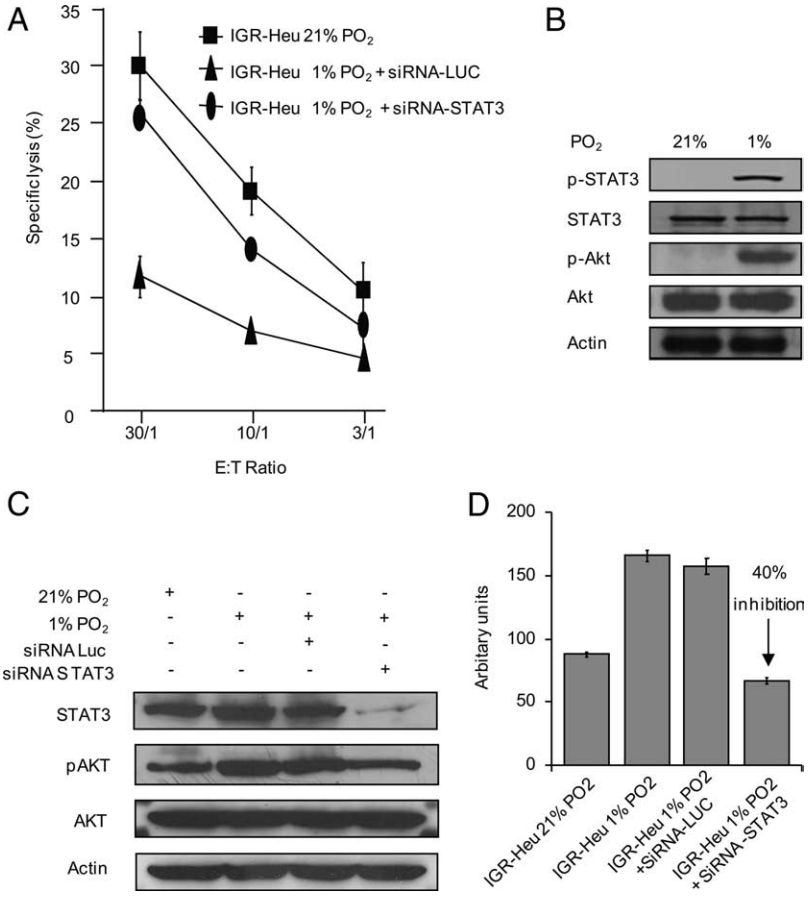

FIGURE 6. Gene silencing of STAT3 results in restoration of IGR-Heu tumor cells susceptibility to CTL (Heu171)-mediated lysis. *A*, Role of STAT3 in Heu171 TIL clone-mediated lysis toward autologous IGR-Heu tumor cells. IGR-Heu tumor cells electroporated with siRNA STAT3 or siRNA-luciferase in normoxia (21% PO_2) and hypoxia (1% PO_2) for 16 h. Cytotoxicity was determined by a conventional 4-h ^{51}Cr release assay at different ratios. Heu171 (TIL-derived T cell clone) was used as effectors. Bars, SD. *B*, IGR-Heu tumor cells were kept in normoxia (21% PO_2) and hypoxia (1% PO_2). After 16 h of incubation, whole-cell lysates (30 μg) were subjected to SDS-PAGE, blotted, and probed with Abs, as indicated. Actin was used as the loading control. *C*, Western blots analysis after the knockdown of STAT3 by SiRNA. *D*, Densitometry analysis of P-AKT inhibition after gene silencing of STAT3. The images were analyzed by Image J.

Fig. 6*A*, a remarkable increase at all the E:T ratios tested in CTL-induced killing of STAT3-siRNA IGR-Heu-transfected cells as compared with control cells was observed. These data strengthen the notion that activation of STAT3 plays an essential part in the acquisition of tumor cell resistance to CTL-induced killing under hypoxic conditions. Because hypoxia is known to induce AKT phosphorylation, we wished to examine its status in hypoxic IGR-Heu cells as well as its putative involvement in STAT3-induced inhibition of tumor cell susceptibility to CTL-induced lysis. Results shown in Fig. 6*B* indicate that hypoxic treatment resulted in the simultaneous phosphorylation of STAT3 and AKT in IGR-Heu cells, suggesting a role of AKT in the resistance of hypoxic IGR-Heu to CTL. As shown in Fig. 6*C*, knocking down of STAT3 in hypoxic cells resulted in down-regulation of p-AKT phosphorylation. As shown in Fig. 6*D*, a significant decrease (40%) in the induction of p-AKT following STAT3 knockdown was observed.

Gene silencing of HIF-1α resulted in restoration of IGR-Heu tumor cells susceptibility to CTL-mediated killing under hypoxic stress.

To delineate the role of HIF-1α in the regulation of tumor cell susceptibility to CTL mediated lysis under hypoxic conditions, siRNA mediated knock down of HIF-1α under hypoxic conditions was performed. As shown in Fig. 7*A*, a strong inhibition of HIF-1α induction (>90%) under hypoxic stress was observed. Using three different siRNA sequences, when these cells were tested for their susceptibility to CTL induced killing, a remarkable restoration of cell lysis was obtained (Fig. 7*B*). This point to a role of HIF-1α in the negative regulation of hypoxic tumor targets susceptibility to lysis by the autologous CTL.

Microarray expression profiles of tumor cells in response to hypoxia: relationship with STAT3

To further investigate the role of HIF-1α and STAT3 in controlling tumor cell susceptibility to lysis by CTL, we performed a global analysis using DNA Microarray (Agilent Human Whole Genome Microarray: 44,000 spots) under two different conditions, hypoxia vs normoxia (Hypo Normo) and siRNA STAT3 vs siRNA-Luc (STAT3 CT). Of 44,000 probe sets, for Hypo Normo, 4138 probe sets were differentially expressed with a 2-fold change: 1582 probe sets were down-regulated and 2556 up-regulated. For (STAT3 CT), we found 354 probe sets that were differentially expressed with a 2-fold change: 88 probe sets were down-regulated and 266 up-regulated. These results are summarized in Fig. 8*A* and point to a potential role of both hypoxia-induced HIF-1α and hypoxia-activated STAT3 in modulating the tumor behavior.

To identify the molecular processes/potential clusters associated with the modulation of tumor cell susceptibility to CTL-mediated lysis, the differentially expressed probe sets were analyzed by Rosetta resolver software. This analysis indicates that the majority of genes differentially expressed under hypoxic conditions belong to five major groups, namely metabolism, apoptosis, cell cycle, cell adhesion, and transcriptional regulation. Similarly, under siRNA STAT3 inhibition condition, the overall profile showed a similar gene ontology distribution. These results further strengthen the role of STAT3 in modulating the hypoxic response (Fig. 8*B*). In addition, as shown in Fig. 8*A*, under (STAT3 CT), the number of differentially expressed genes was reduced and using pathway analysis softwares Rosetta and GenMapp/Mapfinder; these genes were found to be dispersed among a number of pathways and not

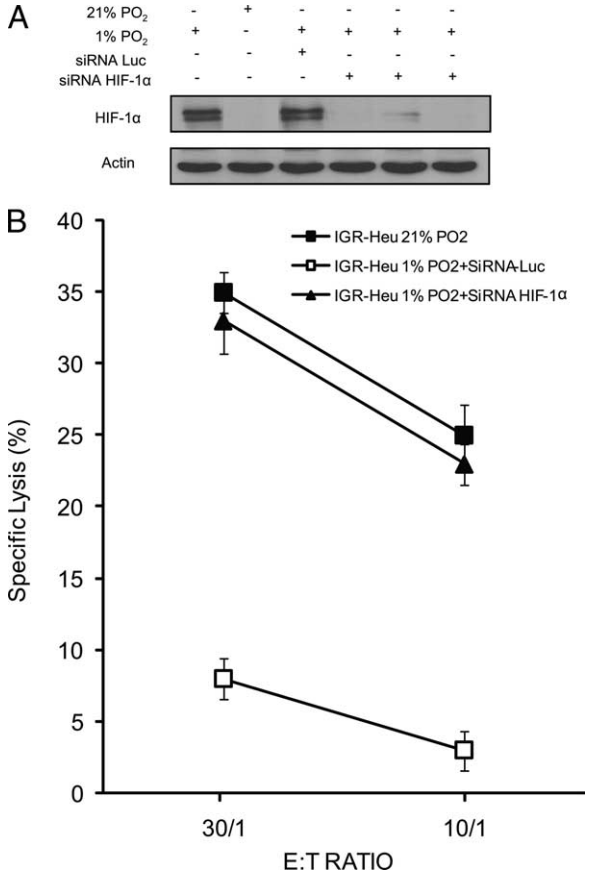

FIGURE 7. Restoration of IGR-Heu tumor cells susceptibility to CTL (Heu171)-mediated lysis following RNAi-mediated gene silencing of HIF-1α under hypoxic conditions. *A*, Gene silencing of HIF-1α under hypoxic conditions. IGR-Heu tumor cells were transfected with siRNA HIF-1α or control siRNA-luciferase. Seventy-two hours after transfection, whole-cell lysates (30 μg) were subjected to SDS-PAGE, blotted, and probed with Abs, as indicated. Actin was used as the loading control. *B*, Role of HIF-1α in modulating tumor cell susceptibility to Heu171-CTL clone-mediated lysis. IGR-Heu tumor cells electroporated with three different siRNA HIF-1α or siRNA-luciferase in hypoxia (1% PO_2) for 16 h. Cytotoxicity was determined by a conventional 4-h ^{51}Cr release assay at different ratios. Heu171 (CTL clone) was used as effectors. Bars SD.

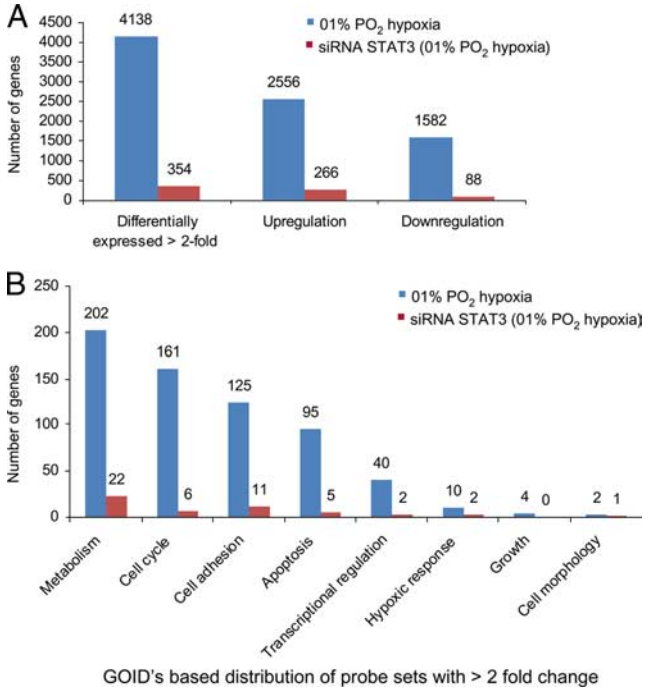

FIGURE 8. Differential gene expression under 1% PO_2 hypoxic and siRNA STAT3 conditions. *A*, IGR-Heu tumor cells were kept under normoxia (21% PO_2) and hypoxia (1% PO_2) for 24 h. Total RNA was isolated, and DNA microarray analysis was performed using an Agilent Human Whole Genome Microarray. *B*, Gene ontology identification (GOID) classification based distribution of probe sets >2-fold change under hypoxic and siRNA STAT3 conditions. Rosetta resolver software was used for analysis.

linked to a single pathway. We further proceeded by making a list of genes that had changed significantly under hypoxia (up or down) and linked it with the expression of the same genes under STAT3 inhibition. These combined results (mHypxmSTAT) indicate that there is a reversal (partial or full) of the expression when STAT3 is inhibited under hypoxia and returning to a normoxic profile. The most prominent changes are listed in Table I with some of the genes in this list related to cell death: AATK, MAF, MAPK4, and MYCT1. Further analysis of the molecular pathways resulted in the identification of an additional list of genes that are known to play a role in regulation of resistance/apoptosis: DFFB, TRIB3, ERN1, BCLAF1, and NALP1. It is interesting to mention here that in the list of differential expressed genes there were also several genes linked to NF-κB signaling.

Taken together, the microarray analysis suggests that hypoxia-induced HIF-1α and p-STAT3 may act coordinately to mediate hypoxia-induced alteration of tumor susceptibility to CTL-mediated lysis.

Discussion

The efficacy of antitumor CTL critically depends on functional processing and presentation of tumor Ags by the malignant cells but also on their susceptibility to CTL-induced lysis. The identification of tumor-associated Ags and their epitopes recognized by autologous T cells has lead to their broad use as immunogens to induce or augment tumor-associated Ag-specific immune responses in vaccination strategies (23, 39–42). However, the understanding of tumor-host interactions remains elusive despite this identification. In fact, tumor rejection in patients does not always follow successful induction of tumor-specific immune responses by cancer vaccine immunotherapy (4). Even if a strong and sustained cytotoxic response is induced, complex issues such as tumor evasion and selection of tumor-resistant variants remain. In this respect, solid tumors with disorganized, insufficient blood supply contain hypoxic cells that are resistant to classical cytotoxic treatments (43). The results of the present studies provide the first demonstration that tumor cells, through their adaptation to hypoxic stress, impede CTL cytotoxic activity independently of their potential to trigger CTL reactivity. However, our data differ from earlier report of MacDonald and Koch (44). This discrepancy may lie in the fact that the reported data were collected using mice system, CTL generated in mixed leukocyte cultures, and hypoxic chambers, whereas we respectively used human Ag-specific CTL clone and hypoxic station. These observations are consistent with the notion that hypoxia-induced adaptive changes contribute to alterations that lend toward a surviving phenotype. Thus, it is conceivable to imagine that tumors frequently develop this specific strategy to shift the balance from immune surveillance to tolerance. In this context, the various strategies aimed at the induction of antitumor cytotoxic responses should consider the crucial role of tumor hypoxia as an additional antitumor mechanism of tumor escape that is partly involved in resistance of tumor cells to Ag-specific cytotoxicity.

Table I. *List of genes that gave a reversal (partial or full) of expression under STAT3 inhibition*[a]

Primary Sequence Name	Accession No.	MeanHYP	MeanSTAT	mHypxmSTAT
AATK[b]	NM_001080395	8.085192508[c]	0.419208371[d]	3.389380384
ABLIM3	NM_014945	6.649144582	0.426638997	2.836784373
ADH1A	NM_000667	0.167966415	2.019030276	0.339129278
ADH1A	NM_000667	0.231080138	2.226025826	0.514390355
ANGPTL4	NM_139314	31.45983155	0.307092850	9.661089326
BNC2	NM_017637	2.349535188	0.479137192	1.125749692
C16orf78	NM_144602	0.501471398	2.068901367	1.037494861
CALB2	NM_001740	33.55977682	0.412261363	13.83539933
CD72	NM_001782	4.753225996	0.403382591	1.917368619
CNN1	NM_001299	2.143496155	0.405801693	0.869834369
EBI3	NM_005755	17.33144061	0.393332038	6.817010850
EFNA1	NM_004428	12.93814775	0.481075561	6.224226688
FGF21	NM_019113	3.191536311	0.328079978	1.047079163
FGG	NM_000509	4.171329662	0.275914383	1.150929851
GLT1D1	NM_144669	7.621011279	0.399096116	3.041515999
HCG4	NR_002139	3.418579404	0.387191733	1.323645684
HMGCLL1	NM_019036	2.456706141	0.408455845	1.003455983
HTR3A	NM_213621	4.450853706	0.434079395	1.932023882
IL21R	NM_181078	7.608334185	0.180035020	1.369766595
JAK3	BC028068	2.418664759	0.444393028	1.074837756
KCNMB4	NM_014505	4.107457716	0.493705933	2.027876243
LCN2	NM_005564	2.432430479	0.317610668	0.772565868
LY96	NM_015364	8.183074746	0.382420550	3.129375943
MAF[b]	AF055376	3.373622120[c]	0.488526477[d]	1.648103730
MAPK4[b]	X59727	60.05014398[c]	0.414925830[d]	24.91635583
MYCT1[b]	NM_025107	3.398289596[c]	0.483077899[d]	1.641638598
NNMT	NM_006169	28.66610466	0.342793814	9.826563336
OR51E2	NM_030774	0.073586722	2.456032870	0.180731407
PECAM1	NM_000442	10.68675702	0.437580990	4.676321721
PLA2G3	NM_015715	3.960428765	0.449291227	1.779385898
PTGS1	NM_000962	5.496247103	0.435281377	2.392414008
SOCS3	NM_003955	30.13365930	0.354334745	10.67740248
SRPX2	NM_014467	4.621833783	0.416867169	1.926690763
STAT3	NM_213662	2.128718329	0.248762483	0.529545258
TNFRSF11A	AB209762	2.400841610	0.487085993	1.169416319
TNS1	NM_022648	9.331115713	0.482862705	4.505647770
TNXB	NM_032470	11.10529609	0.429757704	4.772586553
TSKS	NM_021733	5.177481996	0.324157290	1.678318533
BCLAF1[b]	NM_014739	0.503805042[d]	1.283749270[c]	0.632957814
DFFB[b]	NM_004402	0.430407334[d]	1.201755655[c]	0.518365789
ERN1[b]	AK055561	2.047796458[c]	0.965524773[c]	1.908652475
NALP1=NLRP1[b]	NM_033004	0.557328993[d]	1.288832253[c]	0.708904005
TRIB3[b]	NM_021158	2.175000632[c]	0.783258470[d]	1.704318640

[a] Using GenMAPP2 analysis, a list of genes was created that gave a reversal under STAT3 inhibition. MeanHYP, mean hypoxia in absolute numbers; MeanSTAT, mean STAT inhibition; and meanHYPXSTAT, product meanHYP × meanSTAT should give indication on the expression between normoxic cells and hypoxic cells with STAT inhibition.
[b] Genes related to cell death.
[c] Genes up-regulated.
[d] Genes down-regulated.

To get more insights into the mechanism associated with alteration of tumor susceptibility to CTL-mediated lysis under hypoxic conditions, we asked whether hypoxia resulted in reshaping immunogenicity of tumor cells that may contribute to lose or avoid recognition. We found that hypoxic tumor treatment did not result in alteration of CTL reactivity as measured by TNF secretion and granzyme B polarization, indicating that tumor-induced priming of the autologous CTL clone was not most likely affected after exposure to hypoxia. We further investigated the influence of hypoxia on cell morphology since disruption of the cytoskeletal network by hypoxia has been reported in diverse tissues (45). We did not detect any influence of hypoxia on tumor cell morphological change.

It is well established that hypoxia-induced gene transcription promotes characteristic tumor adaptations, including resistance to cytotoxic treatments. However, the mechanisms underlying this resistance still need a deeper understanding. Although increasing evidence supports a link between hypoxia and resistance to apoptosis (46), the mechanism by which the hypoxic stress inhibits apoptosis is not well understood and remains unclear. In this regard, it has been suggested that alterations in the Bcl-2 family of proapoptotic and antiapoptotic proteins may play a role in this process (47). In addition, HIF-1α-mediated increase in glucose uptake has been also reported to play an important role in conferring apoptosis resistance and that its effect is mediated in part via Mcl-1 gene expression (48). To gain a better understanding of the influence of hypoxia on non-small lung cancer cells' resistance to CTL, we asked whether it interferes with the expression of p53, survivin, AKT, and STAT3 pathways. Under our experimental conditions, we failed to observe any p53 and survivin induction in hypoxic NSCLC, suggesting that the expression of HIF-1α and these proteins may be coupled during the hypoxia response depending on the cell type tested and confirming the existence of a cell-specific effect of hypoxia (49). In the present study, we

demonstrate that culture of IGR-Heu cells under hypoxic conditions resulted in a dramatic induction of STAT3 tyrosine phosphorylation. Moreover, confocal microscopy analysis revealed that the hypoxic cells exhibited an optimal and simultaneous accumulation of HIF-1α and STAT3 in the nucleus. To further delineate the putative interplay between STAT3 and HIF-1α in hypoxia-induced alteration of tumor susceptibility to CTL-mediated cell lysis, we performed experiments to block STAT3 under hypoxic conditions using RNAi. We found that such knockdown resulted in an inhibition of HIF-1α induction. This suggests that STAT3 is an essential component of HIF-1 pathway under hypoxic conditions and fits with a recent report indicating that hypoxia-phosphorylated STAT3 up-regulates HIF-1α stability through delaying protein degradation and accelerating protein synthesis in human renal cell carcinoma (16, 50).

To further elaborate the existing relationship between hypoxia-induced HIF-1α and activated STAT3, using CCB-I, a known inhibitor of STAT3 phosphorylation, we observed that both STAT3 phosphorylation and HIF-1α induction was inhibited in hypoxic tumor cells. These results shown in Fig. 5 strengthen the existing of an interplay between HIF-1α and p-STAT3 during the regulation of specific tumor lysis under hypoxic conditions.

It is also important to note that STAT3 activation has been associated with cytokine-induced proliferation, antiapoptosis, and transformation. We also showed that knockdown of STAT3 in hypoxic IGR-Heu cells resulted in a significant inhibition of AKT phosphorylation (40% inhibition) and significant restoration of tumor susceptibility to CTL, indicating that the attenuation of the resistance of hypoxic cells to CTL-induced cell death may be associated at least in part with inhibition of AKT activation in these cells (Fig. 6*D*). This is also in agreement with our unpublished data indicating that wortmannin, an AKT inhibitor; sensitized tumor cells to CTL-mediated lysis under hypoxic conditions. It should be noted that activated STAT3 in cancer cells does not just function as a mediator of intracellular signaling but also affects cell-cell interaction. In this respect, it is now well established that that STAT3 modulates the cross-talk between tumor and immune cells (36, 51). Very recently, a novel small molecule inhibitor of STAT3 has been reported to reverse immune tolerance in malignant glioma patients (52). It would be of interest to investigate the use of such an inhibitor to attenuate hypoxic tumor resistance to CTL-mediated cytotoxicity.

More interestingly, we have shown that VEGF neutralization resulted in the attenuation of hypoxic tumor target resistance to CTL-mediated killing. We have also demonstrated that STAT3 phosphorylation can be stimulated by autocrine signaling through VEGF, suggesting that tumor microenvironment through hypoxia-induced VEGF may play a key role in the induction of active form of stat3. In this regard, it is very likely that stat3 activation is associated with the regulation of target gene expression potentially involved in the alteration of hypoxic tumor target-specific killing. Therefore, understanding how VEGF and other soluble factors may lead to STAT3 activation via the tumor microenvironment may provide a more effective cancer treatment strategy for hypoxic tumors with elevated p-STAT3 levels. This also suggests that reduction of VEGF release, a main immunosuppressive factor, in tumor microenvironment may favor induction of a stronger anti-tumor CTL response against tumors expressing VEGFR. Our studies are in agreement with reports suggesting that inhibition of VEGF may be a valuable adjuvant in the immunotherapy of cancer (53) and indicating a synergy between tumor immunotherapy and antiangiogenic therapy (54).

The results presented here provide evidence that hypoxia inhibits tumor-specific lysis and suggest that it induces cellular adaptation that compromise the effectiveness of killer cells. Using microarray analysis, we further demonstrate that hypoxia induces transcriptional changes that may promote cell survival and resistance to specific lysis. Cluster analysis of data reveals several possible pathways affected by hypoxia, including apoptosis, cell cycle, metabolism, cell adhesion and transcriptional regulation. Additionally, STAT3 inhibition under hypoxia affected the expression of genes belonging to the same or related pathways and resulted in a partial reversal of the differentially expressed genes under hypoxia. This point to the potential role of STAT3 in tumor adaptation induced by hypoxia. This emphasizes that a better understanding of the tumor behavior and its interplay with the killer cells in the context of the complexity and plasticity of a hypoxic microenvironment will be a critical determinant in a rational approach to tumor immunotherapy. Although resistance of tumor targets to killer cells is likely to be regulated by multiple factors (5), the data we present herein suggest that hypoxic microenvironment is an important determinant involved in the control of target sensitivity to CTL-mediated lysis. Therefore, the possibility that novel approaches targeting HIF-1α and STAT3 with potent small molecule drugs, being actively developed, may provide an exciting novel approach for cancer immunotherapy.

Acknowledgments

We thank Dr. Hua Yu for helpful discussions and Drs. Vladimir Lazar and Philippe Dessen for DNA microarray analysis.

Disclosures

The authors have no financial conflict of interest.

References

1. Rosenberg, S. A. 2001. Progress in the development of immunotherapy for the treatment of patients with cancer. *J. Intern. Med.* 250: 462–475.
2. Lieberman, J. 2003. The ABCs of granule-mediated cytotoxicity: new weapons in the arsenal. *Nat. Rev. Immunol.* 3: 361–370.
3. Trapani, J. A., and M. J. Smyth. 2002. Functional significance of the perforin/granzyme cell death pathway. *Nat. Rev. Immunol.* 2: 735–747.
4. Chouaib, S., C. Asselin-Paturel, F. Mami-Chouaib, A. Caignard, and J. Y. Blay. 1997. The host-tumor immune conflict: from immunosuppression to resistance and destruction. *Immunol. Today* 18: 493–497.
5. Chouaib, S. 2003. Integrating the quality of the cytotoxic response and tumor susceptibility into the design of protective vaccines in tumor immunotherapy. *J. Clin. Invest.* 111: 595–597.
6. Lukashev, D., B. Klebanov, H. Kojima, A. Grinberg, A. Ohta, L. Berenfeld, R. H. Wenger, A. Ohta, and M. Sitkovsky. 2006. Cutting edge: hypoxia-inducible factor 1α and its activation-inducible short isoform I.1 negatively regulate functions of $CD4^+$ and $CD8^+$ T lymphocytes. *J. Immunol.* 177: 4962–4965.
7. Aebersold, D. M., P. Burri, K. T. Beer, J. Laissue, V. Djonov, R. H. Greiner, and G. L. Semenza. 2001. Expression of hypoxia-inducible factor-1α: a novel predictive and prognostic parameter in the radiotherapy of oropharyngeal cancer. *Cancer Res.* 61: 2911–2916.
8. Wang, G. L., B. Jiang, E. A. Rue, and G. L. Semenza. 1995. Hypoxia-inducible factor 1 is a basic-helix-loop-helix-PAS heterodimer regulated by cellular O_2 tension. *Proc. Natl. Acad. Sci. USA* 92: 5510–5514.
9. Wenger, R. H., D. P. Stiehl, and G. Camenisch. 2005. Integration of oxygen signaling at the consensus HRE. *Sci. STKE* 2005: re12.
10. Semenza, G. L. 2000. Chairman's summary: mechanisms of oxygen homeostasis, circa 1999. *Adv. Exp. Med. Biol.* 475: 303–310.
11. Harris, A. L. 2002. Hypoxia—a key regulatory factor in tumour growth. *Nat. Rev Cancer* 2: 38–47.
12. Moeller, B. J., and M. W. Dewhirst. 2004. Raising the bar: how HIF-1 helps determine tumor radiosensitivity. *Cell Cycle* 3: 1107–1110.
13. Unruh, A., A. Ressel, H. G. Mohamed, R. S. Johnson, R. Nadrowitz, E. Richter, D. M. Katschinski, and R. H. Wenger. 2003. The hypoxia-inducible factor-1α is a negative factor for tumor therapy. *Oncogene* 22: 3213–3220.
14. Giaccia, A., B. G. Siim, and R. S. Johnson. 2003. HIF-1 as a target for drug development. *Nat. Rev. Drug Discov.* 2: 803–811.
15. Semenza, G. L. 2003. Targeting HIF-1 for cancer therapy. *Nat. Rev. Cancer* 3: 721–732.
16. Xu, Q., J. Briggs, S. Park, G. Niu, M. Kortylewski, S. Zhang, T. Gritsko, J. Turkson, H. Kay, G. L. Semenza, et al. 2005. Targeting Stat3 blocks both HIF-1 and VEGF expression induced by multiple oncogenic growth signaling pathways. *Oncogene* 24: 5552–5560.
17. Bromberg, J. F., M. H. Wrzeszczynska, G. Devgan, Y. Zhao, R. G. Pestell, C. Albanese, and J. E. Darnell, Jr. 1999. Stat3 as an oncogene. *Cell* 98: 295–303.

18. Catlett-Falcone, R., W. S. Dalton, and R. Jove. 1999. STAT proteins as novel targets for cancer therapy: signal transducer an activator of transcription. *Curr. Opin. Oncol.* 11: 490–496.
19. Bowman, T., M. A. Broome, D. Sinibaldi, W. Wharton, W. J. Pledger, J. M. Sedivy, R. Irby, T. Yeatman, S. A. Courtneidge, and R. Jove. 2001. Stat3-mediated Myc expression is required for Src transformation and PDGF-induced mitogenesis. *Proc. Natl. Acad. Sci. USA* 98: 7319–7324.
20. Germain, D., and D. A. Frank. 2007. Targeting the cytoplasmic and nuclear functions of signal transducers and activators of transcription 3 for cancer therapy. *Clin. Cancer Res.* 13: 5665–5669.
21. Al Zaid Siddiquee, K., and J. Turkson. 2008. STAT3 as a target for inducing apoptosis in solid and hematological tumors. *Cell Res.* 18: 254–267.
22. Dayan, F., D. Roux, M. C. Brahimi-Horn, J. Pouyssegur, and N. M. Mazure. 2006. The oxygen sensor factor-inhibiting hypoxia-inducible factor-1 controls expression of distinct genes through the bifunctional transcriptional character of hypoxia-inducible factor-1α. *Cancer Res.* 66: 3688–3698.
23. Echchakir, H., F. Mami-Chouaib, I. Vergnon, J. F. Baurain, V. Karanikas, S. Chouaib, and P. G. Coulie. 2001. A point mutation in the α-actinin-4 gene generates an antigenic peptide recognized by autologous cytolytic T lymphocytes on a human lung carcinoma. *Cancer Res.* 61: 4078–4083.
24. Dorothee, G., I. Vergnon, F. El Hage, B. Le Maux Chansac, V. Ferrand, Y. Lecluse, P. Opolon, S. Chouaib, G. Bismuth, and F. Mami-Chouaib. 2005. In situ sensory adaptation of tumor-infiltrating T lymphocytes to peptide-MHC levels elicits strong antitumor reactivity. *J. Immunol.* 174: 6888–6897.
25. Echchakir, H., I. Vergnon, G. Dorothee, D. Grunenwald, S. Chouaib, and F. Mami-Chouaib. 2000. Evidence for in situ expansion of diverse antitumor-specific cytotoxic T lymphocyte clones in a human large cell carcinoma of the lung. *Int. Immunol.* 12: 537–546.
26. Lund, E. L., L. T. Hansen, and P. E. Kristjansen. 2005. Augmenting tumor sensitivity to topotecan by transient hypoxia. *Cancer Chemother. Pharmacol.* 56: 473–480.
27. Asselin-Paturel, C., S. Megherat, I. Vergnon, H. Echchakir, G. Dorothee, S. Blesson, F. Gay, F. Mami-Chouaib, and S. Chouaib. 2001. Differential effect of high doses versus low doses of interleukin-12 on the adoptive transfer of human specific cytotoxic T lymphocyte in autologous lung tumors engrafted into severe combined immunodeficiency disease-nonobese diabetic mice: relation with interleukin-10 induction. *Cancer* 91: 113–122.
28. Dorothee, G., H. Echchakir, B. Le Maux Chansac, I. Vergnon, F. El Hage, A. Moretta, A. Bensussan, S. Chouaib, and F. Mami-Chouaib. 2003. Functional and molecular characterization of a KIR3DL2/p140 expressing tumor-specific cytotoxic T lymphocyte clone infiltrating a human lung carcinoma. *Oncogene* 22: 7192–7198.
29. Dasgupta, P., R. Kinkade, B. Joshi, C. Decook, E. Haura, and S. Chellappan. 2006. Nicotine inhibits apoptosis induced by chemotherapeutic drugs by up-regulating XIAP and survivin. *Proc. Natl. Acad. Sci. USA* 103: 6332–6337.
30. Abouzahr, S., G. Bismuth, C. Gaudin, O. Caroll, P. Van Endert, A. Jalil, J. Dausset, I. Vergnon, C. Richon, A. Kauffmann, et al. 2006. Identification of target actin content and polymerization status as a mechanism of tumor resistance after cytolytic T lymphocyte pressure. *Proc. Natl. Acad. Sci. USA* 103: 1428–1433.
31. Diarra-Mehrpour, M., S. Arrabal, A. Jalil, X. Pinson, C. Gaudin, G. Pietu, A. Pitaval, H. Ripoche, M. Eloit, D. Dormont, and S. Chouaib. 2004. Prion protein prevents human breast carcinoma cell line from tumor necrosis factor α-induced cell death. *Cancer Res.* 64: 719–727.
32. Wittnebel, S., A. Jalil, J. Thiery, S. DaRocha, E. Viey, B. Escudier, S. Chouaib, and A. Caignard. 2005. The sensitivity of renal cell carcinoma cells to interferon α correlates with p53-induction and involves Bax. *Eur. Cytokine Netw.* 16: 123–127.
33. Hamai, A., C. Richon, F. Meslin, F. Faure, A. Kauffmann, Y. Lecluse, A. Jalil, L. Larue, M. F. Avril, S. Chouaib, and M. Mehrpour. 2006. Imatinib enhances human melanoma cell susceptibility to TRAIL-induced cell death: relationship to Bcl-2 family and caspase activation. *Oncogene* 25: 7618–7634.
34. Dorothee, G., M. Ameyar, A. Bettaieb, I. Vergnon, H. Echchakir, C. Richon, M. Bouziane, S. Chouaib, and F. Mami-Chouaib. 2001. Role of Fas and granule exocytosis pathways in tumor-infiltrating T lymphocyte-induced apoptosis of autologous human lung-carcinoma cells. *Int. J. Cancer* 91: 772–777.
35. Thiery, J., G. Dorothee, H. Haddada, H. Echchakir, C. Richon, R. Stancou, I. Vergnon, J. Benard, F. Mami-Chouaib, and S. Chouaib. 2003. Potentiation of a tumor cell susceptibility to autologous CTL killing by restoration of wild-type p53 function. *J. Immunol.* 170: 5919–5926.
36. Yu, H., M. Kortylewski, and D. Pardoll. 2007. Crosstalk between cancer and immune cells: role of STAT3 in the tumour microenvironment. *Nat. Rev. Immunol.* 7: 41–51.
37. Lieblein, J. C., S. Ball, B. Hutzen, A. K. Sasser, H. J. Lin, T. H. Huang, B. M. Hall, and J. Lin. 2008. STAT3 can be activated through paracrine signaling in breast epithelial cells. *BMC Cancer* 8: 302.
38. Blaskovich, M. A., J. Sun, A. Cantor, J. Turkson, R. Jove, and S. M. Sebti. 2003. Discovery of JSI-124 (cucurbitacin I), a selective Janus kinase/signal transducer and activator of transcription 3 signaling pathway inhibitor with potent antitumor activity against human and murine cancer cells in mice. *Cancer Res.* 63: 1270–1279.
39. Van den Eynde, B. J., and P. van der Bruggen. 1997. T cell defined tumor antigens. *Curr. Opin. Immunol.* 9: 684–693.
40. Yoshino, I., P. S. Goedegebuure, G. E. Peoples, A. S. Parikh, J. M. DiMaio, H. K. Lyerly, A. F. Gazdar, and T. J. Eberlein. 1994. HER2/neu-derived peptides are shared antigens among human non-small cell lung cancer and ovarian cancer. *Cancer Res.* 54: 3387–3390.
41. Marchand, M., C. J. Punt, S. Aamdal, B. Escudier, W. H. Kruit, U. Keilholz, L. Hakansson, N. van Baren, Y. Humblet, P. Mulders, et al. 2003. Immunisation of metastatic cancer patients with MAGE-3 protein combined with adjuvant SBAS-2: a clinical report. *Eur. J. Cancer* 39: 70–77.
42. Thurner, B., I. Haendle, C. Roder, D. Dieckmann, P. Keikavoussi, H. Jonuleit, A. Bender, C. Maczek, D. Schreiner, P. von den Driesch, et al. 1999. Vaccination with mage-3A1 peptide-pulsed mature, monocyte-derived dendritic cells expands specific cytotoxic T cells and induces regression of some metastases in advanced stage IV melanoma. *J. Exp. Med.* 190: 1669–1678.
43. Albini, A., and M. B. Sporn. 2007. The tumour microenvironment as a target for chemoprevention. *Nat. Rev. Cancer* 7: 139–147.
44. MacDonald, H. R., and C. J. Koch. 1977. Energy metabolism and T cell-mediated cytolysis. I. Synergism between inhibitors of respiration and glycolysis. *J. Exp. Med.* 146: 698–709.
45. Lee, A., J. S. Morrow, and V. M. Fowler. 2001. Caspase remodeling of the spectrin membrane skeleton during lens development and aging. *J. Biol. Chem.* 276: 20735–20742.
46. Volm, M., and R. Koomagi. 2000. Hypoxia-inducible factor (HIF-1) and its relationship to apoptosis and proliferation in lung cancer. *Anticancer Res.* 20: 1527–1533.
47. Erler, J. T., C. J. Cawthorne, K. J. Williams, M. Koritzinsky, B. G. Wouters, C. Wilson, C. Miller, C. Demonacos, I. J. Stratford, and C. Dive. 2004. Hypoxia-mediated down-regulation of Bid and Bax in tumors occurs via hypoxia-inducible factor 1-dependent and -independent mechanisms and contributes to drug resistance. *Mol. Cell. Biol.* 24: 2875–2889.
48. Liu, X. H., E. Z. Yu, Y. Y. Li, and E. Kagan. 2006. HIF-1α has an anti-apoptotic effect in human airway epithelium that is mediated via Mcl-1 gene expression. *J. Cell. Biochem.* 97: 755–765.
49. Semenza, G. L. 2002. Signal transduction to hypoxia-inducible factor 1. *Biochem. Pharmacol.* 64: 993–998.
50. Jung, J. E., H. G. Lee, I. H. Cho, D. H. Chung, S. H. Yoon, Y. M. Yang, J. W. Lee, S. Choi, J. W. Park, S. K. Ye, and M. H. Chung. 2005. STAT3 is a potential modulator of HIF-1-mediated VEGF expression in human renal carcinoma cells. *FASEB J.* 19: 1296–1298.
51. Wang, T., G. Niu, M. Kortylewski, L. Burdelya, K. Shain, S. Zhang, R. Bhattacharya, D. Gabrilovich, R. Heller, D. Coppola, et al. 2004. Regulation of the innate and adaptive immune responses by Stat-3 signaling in tumor cells. *Nat. Med.* 10: 48–54.
52. Hussain, S. F., L. Y. Kong, J. Jordan, C. Conrad, T. Madden, I. Fokt, W. Priebe, and A. B. Heimberger. 2007. A novel small molecule inhibitor of signal transducers and activators of transcription 3 reverses immune tolerance in malignant glioma patients. *Cancer Res.* 67: 9630–9636.
53. Gabrilovich, D. I., T. Ishida, S. Nadaf, J. E. Ohm, and D. P. Carbone. 1999. Antibodies to vascular endothelial growth factor enhance the efficacy of cancer immunotherapy by improving endogenous dendritic cell function. *Clin Cancer Res.* 5: 2963–2970.
54. Nair, S., D. Boczkowski, B. Moeller, M. Dewhirst, J. Vieweg, and E. Gilboa. 2003. Synergy between tumor immunotherapy and antiangiogenic therapy. *Blood* 102: 964–971.